Annual Progress Monitoring **Second Year Report**

University of BRISTOL

June 01, 2018

Dark Matter searches at CMS at $\sqrt{s} = 13$ TeV

Eshwen Bhal

University of Bristol, United Kingdom

Contact information: **eshwen.bhal@bristol.ac.uk**; **eshwen.bhal@cern.ch**

Supervisor: Henning Flaecher (**Henning.Flacher@cern.ch**)

Abstract

This document outlines the progress I have made during the second year of my PhD. In the past year, I have contributed to the α_{T} analysis in CMS in a search for natural and split supersymmetry. As an extension, I have analysed simplified supersymmetric models involving top squarks for the accompanying supplementary material. Since concluding this chapter, my recent work has been devoted to two new analyses: a search for dark matter from semi-visible jet final states; and a combined Higgs boson to invisible state analysis utilising several, distinct Higgs production modes. To attain authorship in the CMS collaboration, I have performed service tasks. As well as continuing to derive jet energy corrections, I have conducted $E_{\mathrm{T}}^{\mathrm{miss}}$ studies, and undertaken Level-1 Trigger shifts and Calorimeter Layer-2 on-call shifts. For my thesis, I intend to include material from the two new analyses mentioned above, and possibly the supersymmetry work as a dark matter interpretation.

Contents

Figures

1 Introduction

The observable universe contains a major component that is not explained by conventional Standard Model (SM) physics. Making up approximately 25.8% of the energy density of the universe [1], the astrophysical evidence suggests that there exists a massive, neutral constituent that has a significant gravitational influence on the visible matter we observe. Labelled "dark matter", this entity has captured the interest of many scientists. Those in particle physics have developed theories and experimental searches in an attempt to understand the characteristics of dark matter.

Dark matter was thought to be created in the hot, early universe when the thermal background allowed its spontaneous pair production. When the universe expanded and cooled, a thermal freeze out occurred: the average temperature became too low to allow significant production [2]. Matter became further separated and the dark matter annihilation rate decreased, leaving a "thermal relic". These remaining particles were attracted via gravity, the only known force by which dark matter interacts. They formed filaments throughout the universe, and the potential wells they induced allowed the progenitors of galaxies to form within.

Although dark matter cannot be directly studied with conventional astronomy, there are several independent astrophysical observations that suggest its existence. The rotation curves of most galaxies are roughly flat [3], contrary to the expected Keplerian curve ($v \propto 1/\sqrt{r}$) from solely baryonic matter. On the galactic scale, dark matter is sprinkled in a roughly spherical halo that spans beyond the observable disc. The inclusive dark matter mass increases linearly [4] to compensate for the decline expressed by visible matter [5, 6]. Weak gravitational lensing of galaxies can cause images to appear distorted from dark matter between the galaxy and observer warping its local spacetime [7].

From these observations, several properties of dark matter can be inferred. It is electrically neutral as it does not interact with light. It is "cold" (non-relativistic), implying its rest mass energy is much greater than the thermal background in the universe. Current estimates suggest its mass is at the GeV or TeV scale [8–10]. If it were on the neutrino scale – and therefore relativistic – it would be too diffuse to condense and allow galaxy formation. This supports the idea of "bottom-up" structure formation in the universe; smaller galaxies form around dark matter clumps, then merge to form larger structures [11]. This also asserts that dark matter is stable, at least on the timescale of the age of the universe.

1.1 Overview of dark matter searches

Whilst all current evidence has been astrophysical, determining the properties of dark matter falls into the realm of particle physics. Of the three types of dark matter searches, its production from high-energy collisions is being probed at the LHC. Protons are collided at energies sufficient to produce the heavy particles that existed in the high-temperature early universe. The CMS experiment utilises its general purpose detector to allow physicists to search for dark matter in different theoretical frameworks.

Despite the Standard Model (SM) providing precise predictions of three of the four fundamental forces and the particles that they interact with, it does not substantiate

the existence of dark matter. Several theories that are beyond (BSM), or extend, the Standard Model can accommodate dark matter candidates such as sterile neutrinos [12], axions [13], and Kaluza-Klein states [14].

I have so far searched for dark matter in the context of supersymmetry (SUSY) [15]. The theory introduces a spin symmetry that predicts a fermionic superpartner for each boson, and vice versa. If the lightest supersymmetric particle (LSP) is stable and electrically neutral, it would provide a promising dark matter candidate. Expected SUSY particle decays produce the LSP and, typically, hadronic jets because of the initial state particles. As LSPs are undetectable, a reconstructed event from a detector would show a momentum imbalance. It contains "missing" transverse energy (MET, $E_{\mathrm{T}}^{\mathrm{miss}}$) which is required to satisfy energy and momentum conservation. So the characteristics of SUSY in a collider would be high $E_{\mathrm{T}}^{\mathrm{miss}}$ from the LSPs, and several jets. But as no hint of supersymmetry has been found, other theories and simplified models from more complete theories have been considered. These are discussed later on.

There is significant motivation to study dark matter from a wider, as well as a more personal, viewpoint. It is important to understand how the universe operates, and dark matter opens up the potential for new physics that improves our understanding of nature. My personal interests include the blend of particle physics and astrophysics, and the opportunity to discover and add to humanity's collective wisdom. With a projected 130 fb^{-1} from the LHC's Run-2 at a centre-of-mass energy $\sqrt{s} = 13$ TeV, there is great potential to constrain some of the properties of dark matter.

2 Research and analysis

My research so far has included the examination of several BSM models. These include searches for natural and split supersymmetry, the presence of a hidden sector containing a dark force resembling QCD, and the potential new physics contributing to the branching fraction of the invisible decay of the Higgs boson.

2.1 Searches for natural and split supersymmetry (long-lived particles)

Most searches for supersymmetry use simplified models that obey "naturalness". Natural supersymmetry necessitates only minimal fine-tuning of the bare Higgs boson mass, and requires only top squarks, bottom squarks, the gluino and lightest neutralino (the LSP in this case) to have masses around the electroweak scale [16]. Whilst these models have reasonable motivation – especially since the discovery of the Higgs boson at a mass of 125 GeV [17] – no hint of natural supersymmetry has been observed. New models have therefore been proposed, such as split supersymmetry. This alternative still includes a dark matter candidate and some other appealing features of its natural counterpart, but decouples all SUSY particles except the gluino and LSP to high energies inaccessible by the LHC. The decay of the gluino is then suppressed by these highly virtual states, allowing it to decay a significant distance from the primary vertex. This is known as a long-lived particle.

An analysis I was involved in searched for both natural and split supersymmetry (see Ref. [18]). My work for the paper and analysis note included the production and analysis of some of our signal models, event visualisation of data at high $H_{\mathrm{T}}^{\mathrm{miss}}$ (missing transverse energy calculated from hadronic particles) for validation purposes, and work on signal model cut flow tables.

My most substantial contribution has been the analysis of extra signal models that were not included in the original interpretation. These are natural models that include top squark (colloquially known as the "stop") production with masses ranging from 250-800 GeV, and mass splittings between it and the LSP of 10-80 GeV. The first model, named "T2tt-4bd", involves the stop decaying into a b quark, two fermions and the LSP: $p \to \tilde{t}\bar{\tilde{t}},\ \tilde{t} \to b\mathrm{f}\bar{\mathrm{f}}\tilde{\chi}_1^0$. The second model T2bW_X05 is similar, but involves the intermediate production of the lightest chargino that decays into a W boson and LSP: $p \to \tilde{t}\bar{\tilde{t}},\ \tilde{t} \to b\tilde{\chi}^{\pm} \to bW^{\pm}\tilde{\chi}_1^0$. The chargino is a linear combination of the wino (superpartner of the W) and charged higgsino (superpartner of the Higgs). The discovery of a 125 GeV Higgs boson lends motivation to this model being studied over the previous one.

The study of these two models was comprised of flat tree production and analysis identical to the signal models in the paper. This included creating the limit plots (Figs. 1, 2), the tables of dominant systematic uncertainties, the observed and expected upper limits of the production cross section, the signal acceptance $\times$ efficiency planes, and plots of the signal overlaid on the predicted background for the benchmark models.

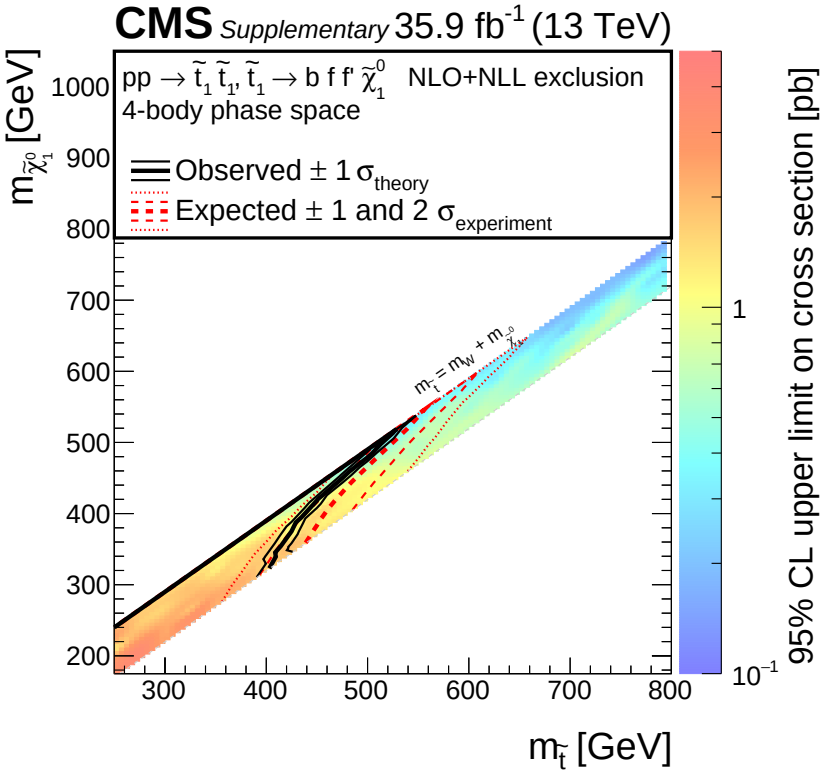

Figure 1: T2tt-4bd: Upper limit on the cross section in the mass plane. The contours reveal the observed and expected exclusions based on the analysis performed.

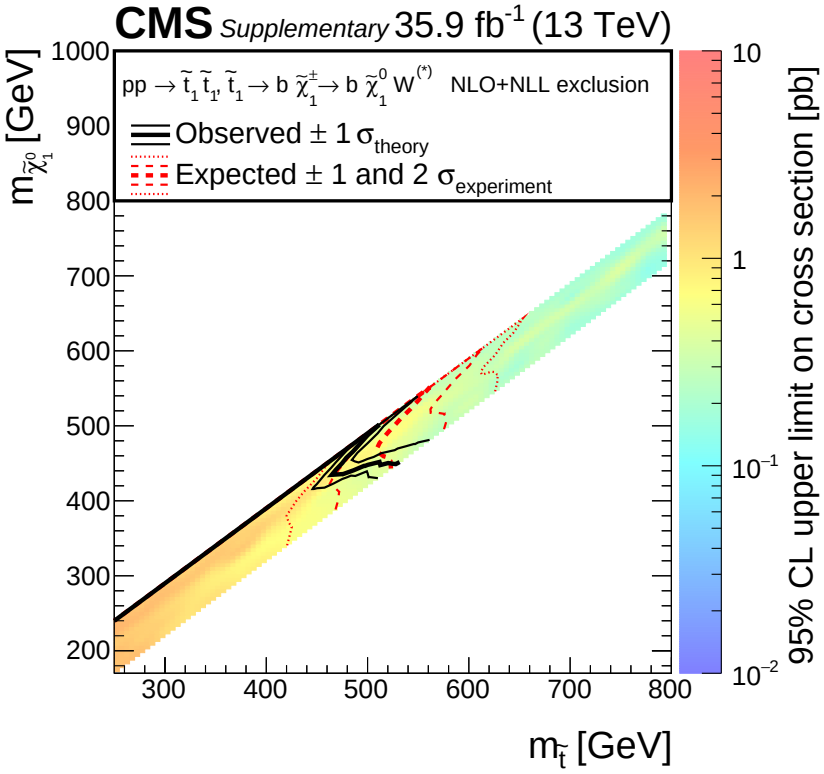

Figure 2: T2bW_X05: Upper limit on the cross section in the mass plane. The contours reveal the observed and expected exclusions based on the analysis performed.

An approval talk was given in a SUSY inclusive meeting for the T2tt-4bd model, where they suggested to analyse the T2bW_X05 as well. An initial comparison to the previous analysis (Fig. 8 in Ref. [19]) indicates an improved limit for each model. Once the cross section reweighting has been performed, required due to generator-level cuts when producing the samples, the material for each of these models will be displayed on the public webpage supplementing the paper.

2.2 Searches for semi-visible jets

After work on the above supersymmetry analysis had concluded and the paper submitted, I became involved in a new prospective analysis searching for dark matter. This search aims to identify dark matter as an invisible component within a hadronic jet, a so-called "semi-visible" jet. The theoretical and experimental motivations behind this final state have been explored in Refs. [20, 21]. The authors postulate a Hidden Valley model [22], where the hidden sector contains a dark QCD-esque force in which dark quarks are produced from the decay of the mediator. Below some dark confinement scale Λ_d, they can hadronise to form a dark jet. Depending on the symmetries of the encapsulating theory, some fraction of the dark hadrons will be stable, yielding MET in a collider event. The remaining fraction will decay into Standard Model hadrons through a portal, governed by an s-channel Z' or t-channel Φ mediator. As depicted in Fig. 3, the MET from the stable dark sector states can be aligned with the jet. Though with higher jet multiplicity, the momentum from the invisible particles can cancel such

that the MET is not aligned with a single jet. These final states are not well-explored in CMS as they can mimic mismeasured QCD events.

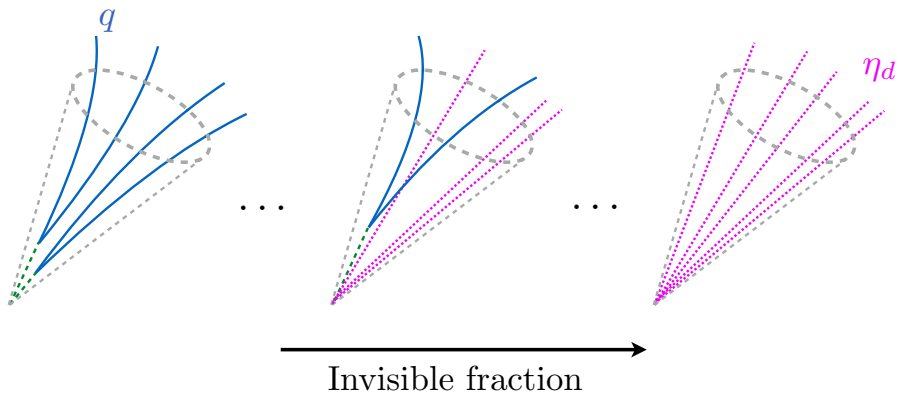

Figure 3: An illustration of semi-visible jets with varying fractions of Standard Model quarks (blue) produced from unstable dark hadrons (green), and an invisible component (pink), lifted from Ref. [21]. As it is difficult to discern each individual constituent in a shower of this nature, the entire jet is clustered and more general properties must be analysed.

Experimentally, the models exhibiting these processes can be characterised by the following parameters: the running dark coupling α_d, the dark quark mass m_d, the mediator mass m_{med}, the fraction of stable dark hadrons r_{inv}, and the dark confinement scale Λ_d related to the coupling via

$$\Lambda_d = 1000\ [\text{GeV}] e^{\frac{-2\pi}{\alpha_d b}} \tag{1}$$

where $b = \frac{11}{3}N_c - \frac{2}{3}N_f$ is related to the number of dark colours and number of flavours [21].

After initially collaborating with physicists at Universität Zürich, we were approached by a group from Fermilab and Rochester who proposed combining our efforts into a single analysis. Though still in its early stages, we have a basic analysis strategy in which we are refining signal Monte Carlo sample production, have defined a preliminary signal region and event preselection, have estimations of dominant backgrounds and are studying discriminating variables.

My involvement in this undertaking has been, primarily, to produce signal samples. The Fermilab group has produced s-channel samples using PYTHIA8 [23], but the theorists recommend MADGRAPH5_AMCATNLO [24] as the generator, especially for the t-channel process. They provided preliminary UFO model files which I have edited in order to perform parameter scans. I have developed a workflow in which the user specifies some model parameters in a config file, which is parsed by Python scripts that create a gridpack (required for eventual central production) of the MADGRAPH release and input files. The output LHE file is run through the PYTHIA hadroniser with acting Hidden Valley processes and GEANT4 detector simulation [25], all inside the CMS SoftWare environment. My configuration is currently set to emulate Monte Carlo produced in 2016 with re-processing in 2017. The s-channel process has been

well-understood but the t-channel not so. These are both UV completions [26] of the contact operator from resolving at tree level and are interesting to include in their own right. Individually, they may exhibit features that can be probed, and together will definitely prove to be a unique analysis. My future tasks will likely be understanding the t-channel process and analysing the models once mature samples have been produced.

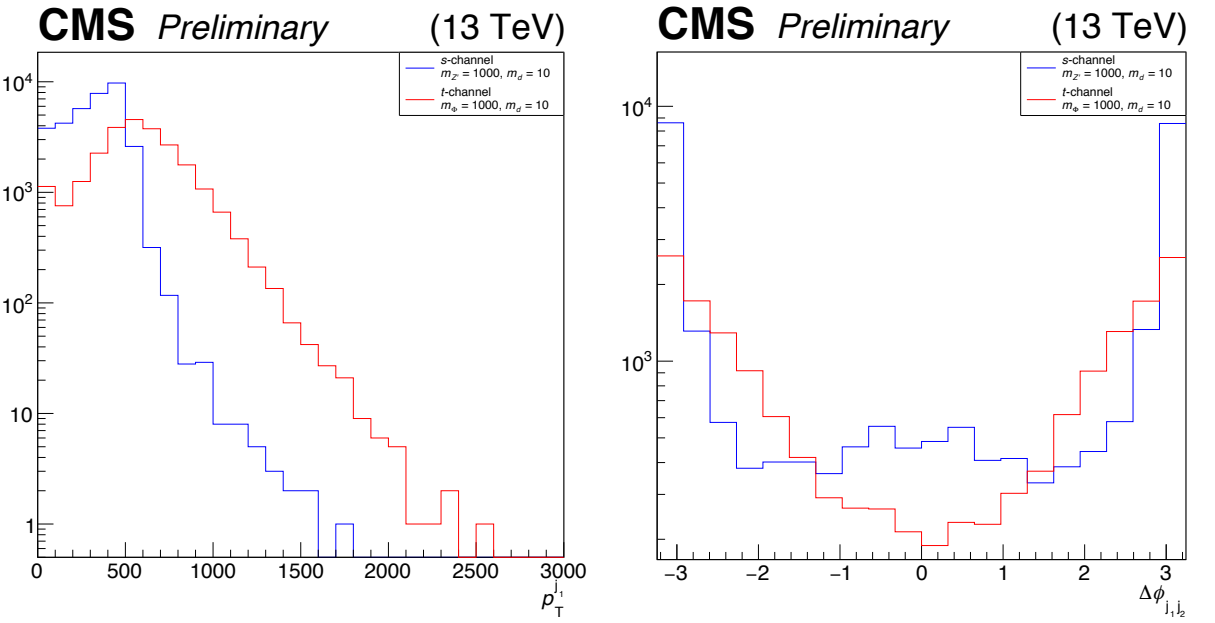

(a) The leading jet p_{T}

(b) $\Delta\phi$ between the leading and sub-leading jet

Figure 4: Histograms comparing two potential discriminating variables in the search for semi-visible jets. The s- and t-channel models with the following parameters are compared: $m_{\mathrm{med}} = 1000$ GeV, $m_d = 10$ GeV, $\Lambda_d = 10.5$ GeV and $r_{\mathrm{inv}} = 0.3$.

The plots in Fig. 4 depict distributions of two variables that illustrate the kinematics of the s- and t-channel models. These were produced after running my complete sample production workflow, i.e., the objects are reconstructed. For the leading jet p_{T}, the peak corresponds to roughly half the mediator mass. This is expected in the case of di-jet events that contain few dark particles. Plots of the number of jets and the $E_{\mathrm{T}}^{\mathrm{miss}}$ corroborate this (see Appendix A). The jet multiplicity can be high, but with a large fraction of soft jets. $E_{\mathrm{T}}^{\mathrm{miss}}$ histograms peak at low energy which is expected when r_{inv} is low. Fig. 4b exhibits peaks at $\Delta\phi = \pm\pi$, suggesting a large proportion of events contain back-to-back jets. For the s-channel model a smaller peak arises around zero. This implies two hard jets produced that recoil from either many soft particles or stable dark hadrons. The interpretations of these plots help verify the models and parameters that have been implemented.

2.3 Combined $H \rightarrow$ inv. analysis

Whilst working on semi-visible jets, I am also involved in a combined Higgs to invisible analysis. This is "combined" in the sense that we will perform a Higgs $\rightarrow$ inv. search over all possible SM production modes in a single analysis. This is in contrast to the regular approach in which a separate analysis would be conducted for each channel and

results would be combined at the end. Our strategy should give much better sensitivity than has previously been possible.

Despite this analysis seeming purely Standard Model-based, there is the possibility to explore new physics. The branching fraction for $H \to \nu\nu$ is predicted to be approximately 1% [27]. However, the current experimental limit on this value is 24% [28]. If the Higgs couples to new, exotic particles, this branching ratio should increase as the coupling is related to the mass of the particle. If we are able to close the gap between the theoretical and experimental values, it may prove to be a powerful constraint on new physics models. Once the analysis has been finalised, new models can be considered such as those involving dark matter.

A subset of the Higgs production modes we are considering are gluon-gluon fusion (ggF), top pair production with a Higgs (ttH), Higgs production in association with a vector boson (VH), and vector boson fusion (VBF). Feynman diagrams are displayed in Appendix B. Our first step is to analyse samples from each of these processes and attempt to construct orthogonal signal regions to cover the largest phase space possible. An analysis will then be performed to extract the limit on the invisible (neutrino) branching fraction. As these processes are Standard Model and not BSM, this is a simpler undertaking in the sense it does not involve parameter scans or any other nuisances that arises from those models. My current task is to investigate ttH sample production, binning it and exploring discriminating variables. In the future, it may develop into analysing dark matter models in this context, if we decide on pursuing BSM physics.

3 Service work

In addition to analysis, researchers that are a part of CMS must undertake service work, or Experimental Physics Responsibility. These are normally maintenance-based tasks related to the detector or infrastructure that keep the experiment running smoothly. My service work has included jet energy corrections (JECs) in Layer-2 of the calorimeter in the Level-1 (L1) Trigger, high-MET studies of trigger primitives, and shift work.

3.1 Jet Energy Corrections in the Level-1 Trigger

JECs are necessary to compensate for various losses when recording jet properties in the trigger. These losses depend on the transverse momentum p_{T} and pseudorapidity η. The calibrations ensure that the performance of the trigger is uniform across the detector. Firstly, some ideal (or reference) jets are needed to compare against given L1 jets. Since Monte Carlo datasets are used for the calibrations, the reference jets we use are GenJets. These are stable, simulated particles clustered with the anti-k_t algorithm [29] to form the jet. The state of these jets are post-hadronisation, before detector interaction. L1 jets need to be matched against the GenJets. From there, various studies can be performed such measuring the response ($< p_{\mathrm{T}}^{\mathrm{L1}}/p_{\mathrm{T}}^{\mathrm{ref.}} >$) of the detector, and its position and energy resolutions.

Once Calorimeter Layer-1 experts have derived scale factors for the physics objects, they are applied in Layer-2 where the calibrations are conducted. For jets, ntuples are

created from the specified dataset and the L1 jets are matched to the GenJets using the variable ΔR:

$$\Delta R = \sqrt{\Delta\eta^2 + \Delta\phi^2} \tag{2}$$

where ϕ is the azimuthal angle of the jet. The algorithm used to match the jets does so by inspecting each L1 jet in descending p_{T} and searching for a reference jet with $\Delta R < 0.25$. If there is more than one match, the reference jet with the smallest ΔR is taken. Then the next L1 jet (and so on) follows the same procedure, with the previous reference jet removed from the matching collection. Calibrations are then derived. Graphs of 1/response vs. $p_{\mathrm{T}}^{\mathrm{L1}}$ are plotted for each $|\eta|$ bin and correction curves are fitted to them (Fig. 5). Once tuned such that the fit captures the low-p_{T} spike and high-p_{T} plateau, closure tests are conducted as the final step. The ntuples are remade with JECs and then matched with the reference jets to check that the calibrations have been properly applied. Plots such as Fig. 6 are then passed to the Trigger Studies Group to check over and continue the chain of trigger corrections and object calibrations.

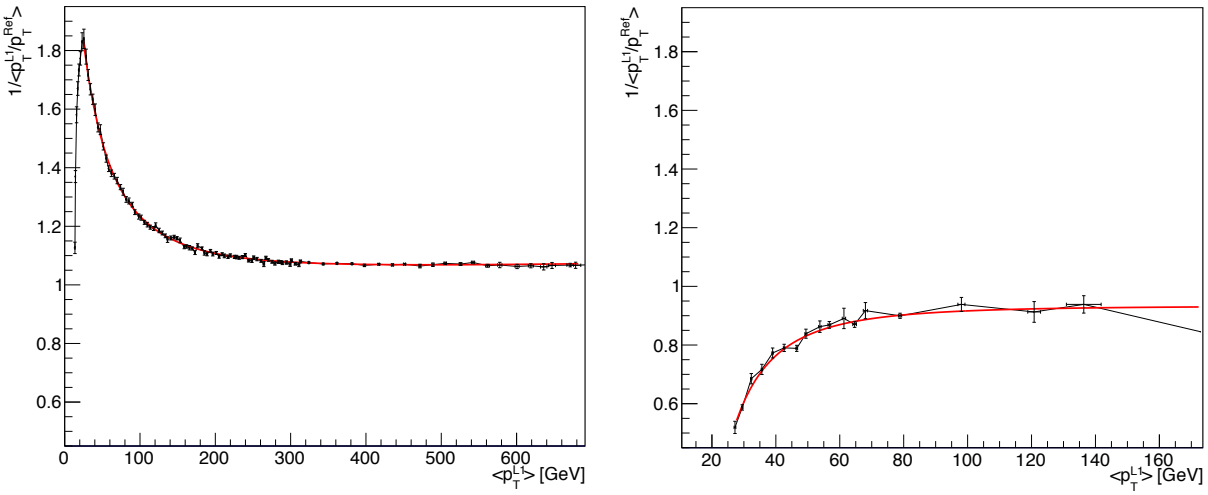

(a) $0.435 < |\eta| < 0.783$ (Barrel)

(b) $4.191 < |\eta| < 5.191$ (HF)

Figure 5: Examples of correction curves used to calibrate the jet energies in two $|\eta|$ bins. The response is plotted against the p_{T} of the Level-1 jet and a complex function produces a fit. These plots are from the jet energy corrections performed on 2018 QCD Monte Carlo.

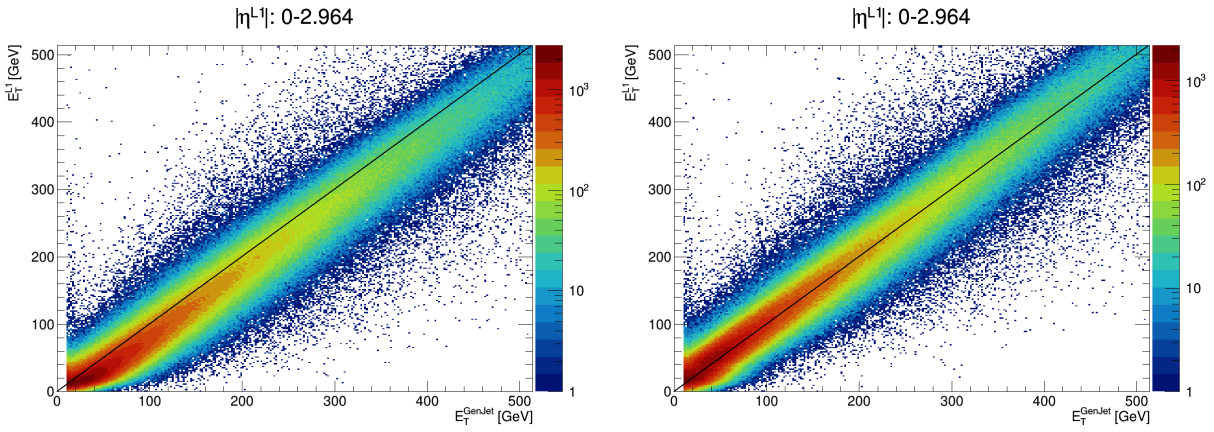

(a) Before corrections

(b) After corrections

Figure 6: Scatter plots showing the energies of matched pairs of jets in the entire barrel and end cap, before and after jet energy corrections have been applied. After calibrations, the distribution is much more symmetrical. An equivalent plot using jets from LHC data is expected to look similar after applying these calibrations.

3.2 Other tasks

In addition to JECs, I have performed on-call shifts for Calorimeter Layer-2, Level-1 Trigger shifts at Point 5, and trigger primitive (TP) studies in high-MET events in ZeroBias data [30]. These studies had the purpose of checking whether there are obvious issues with hot towers, ECAL spikes, pileup mis-estimation, and more. I made plots of various properties from TPs in ECAL, HCAL and the entire trigger tower. These have been featured and discussed in several meetings regarding the status of the TPs and how to deal with the hot trigger tower 28.

Presenting is the main avenue to showcase my work on the trigger. I have given several talks about JECs and a CMS Week presentation on the status of the jet and MET triggers in 2017 with plans for 2018. I am scheduled to present a poster on the jet and energy sum triggers for Run-2 of the LHC at the LHCP conference in June.

4 Thesis outline and future research

My overall research goals are to perform complete analyses for Higgs to invisible and semi-visible jets with my respective analysis groups. For my thesis, the aim is to conduct dark matter interpretations with, ideally, the full 2016-2017 datasets with the Higgs to invisible analysis, and full 2016-2018 datasets with the semi-visible jets analysis.

In the shorter term, I will be attending the LHCP conference in June of this year, and the AEPSHEP summer school in September. After returning from my long term attachment of CERN in April 2019, my time will be dedicated much more to analysis. My service responsibilities should be reduced as the focus turns to my thesis, which I expect to submit around March 2020. The completion of these aforementioned goals will hopefully lead to a comprehensive experimental PhD and a contribution to the field of particle physics in pursuit of understanding dark matter.

References

[1] Planck Collaboration et al. "Planck 2015 results. XIII. Cosmological parameters". In: *Astronomy & Astrophysics* 594, A13 (Sept. 2016), A13. DOI: 10.1051/0004-6361/201525830. arXiv: 1502.01589.

[2] Iason Baldes and Kalliopi Petraki. "Asymmetric thermal-relic dark matter: Sommerfeld-enhanced freeze-out, annihilation signals and unitarity bounds". In: (2017). arXiv: 1703.00478 [hep-ph].

[3] M. Persic, P. Salucci, and F. Stel. "The universal rotation curve of spiral galaxies - I. The dark matter connection". In: *Monthly Notices of the Royal Astronomical Society* 281 (July 1996), pp. 27–47. DOI: 10.1093/mnras/281.1.27. eprint: astro-ph/9506004.

[4] J. Einasto. "Dark Matter". In: *ArXiv e-prints* (Jan. 2009). arXiv: 0901.0632 [astro-ph.CO].

[5] K. C. Freeman. "On the Disks of Spiral and S0 Galaxies". In: *The Astrophysical Journal* 160 (June 1970), p. 811. DOI: 10.1086/150474.

[6] A. H. Broeils. "The mass distribution of the dwarf spiral NGC 1560". In: *Astronomy & Astrophysics* 256 (Mar. 1992), pp. 19–32.

[7] D. Huterer. "Weak lensing, dark matter and dark energy". In: *General Relativity and Gravitation* 42 (Sept. 2010), pp. 2177–2195. DOI: 10.1007/s10714-010-1051-z. arXiv: 1001.1758 [astro-ph.CO].

[8] Steven Lowette. "Search for Dark Matter at CMS". In: *Nucl. Part. Phys. Proc.* 273-275 (2016), pp. 503–508. arXiv: 1410.3762 [hep-ex].

[9] Vasiliki A Mitsou. "Overview of searches for dark matter at the LHC". In: *Journal of Physics: Conference Series* 651.1 (2015), p. 012023.

[10] Tae Min Hong. "Dark matter searches at the LHC". In: *5th Large Hadron Collider Physics Conference (LHCP 2017) Shanghai, China, May 15-20, 2017*. 2017. arXiv: 1709.02304 [hep-ex].

[11] S. D. M. White and M. J. Rees. "Core condensation in heavy halos: a two-stage theory for galaxy formation and clustering". In: *Monthly Notices of the Royal Astronomical Society* 183.3 (1978), p. 341. DOI: 10.1093/mnras/183.3.341.

[12] Marco Drewes. "The Phenomenology of Right Handed Neutrinos". In: *International Journal of Modern Physics E* 22.08 (2013), p. 1330019. DOI: 10.1142/S0218301313300191.

[13] M. Dine, W. Fischler, and M. Srednicki. "A simple solution to the strong CP problem with a harmless axion". In: *Physics Letters B* 104 (Aug. 1981), pp. 199–202. DOI: 10.1016/0370-2693(81)90590-6.

[14] Tao Han, Joseph D. Lykken, and Ren-Jie Zhang. "On Kaluza-Klein states from large extra dimensions". In: *Phys. Rev.* D59 (1999), p. 105006. DOI: 10.1103/PhysRevD.59.105006. arXiv: hep-ph/9811350 [hep-ph].

[15] Stephen P. Martin. "A Supersymmetry primer". In: (1997). [Adv. Ser. Direct. High Energy Phys.18,1(1998)]. DOI: 10.1142/9789812839657_0001, 10.1142/9789814307505_0001. arXiv: hep-ph/9709356 [hep-ph].

[16] J. Alberto Casas et al. "What is a Natural SUSY scenario?" In: *JHEP* 06 (2015), p. 070. DOI: 10.1007/JHEP06(2015)070. arXiv: 1407.6966 [hep-ph].

[17] Serguei Chatrchyan et al. "Observation of a new boson at a mass of 125 GeV with the CMS experiment at the LHC". In: *Phys. Lett.* B716 (2012), pp. 30–61. DOI: 10.1016/j.physletb.2012.08.021. arXiv: 1207.7235 [hep-ex].

[18] A. M. Sirunyan and etal. "Search for natural and split supersymmetry in proton-proton collisions at $\sqrt{s} = 13$ TeV in final states with jets and missing transverse momentum". In: *Journal of High Energy Physics* 2018.5 (May 2018), p. 25. DOI: 10.1007/JHEP05(2018)025.

[19] Vardan Khachatryan et al. "A search for new phenomena in pp collisions at $\sqrt{s} = 13$ TeV in final states with missing transverse momentum and at least one jet using the α_{T} variable". In: *Eur. Phys. J.* C77.5 (2017), p. 294. DOI: 10.1140/epjc/s10052-017-4787-8. arXiv: 1611.00338 [hep-ex].

[20] Timothy Cohen, Mariangela Lisanti, and Hou Keong Lou. "Semi-visible Jets: Dark Matter Undercover at the LHC". In: *Phys. Rev. Lett.* 115.17 (2015), p. 171804. DOI: 10.1103/PhysRevLett.115.171804. arXiv: 1503.00009 [hep-ph].

[21] Timothy Cohen et al. "LHC Searches for Dark Sector Showers". In: *JHEP* 11 (2017), p. 196. DOI: 10.1007/JHEP11(2017)196. arXiv: 1707.05326 [hep-ph].

[22] Matthew J. Strassler and Kathryn M. Zurek. "Echoes of a hidden valley at hadron colliders". In: *Phys. Lett.* B651 (2007), pp. 374–379. DOI: 10.1016/j.physletb.2007.06.055. arXiv: hep-ph/0604261 [hep-ph].

[23] Torbjorn Sjostrand, Stephen Mrenna, and Peter Z. Skands. "A Brief Introduction to PYTHIA 8.1". In: *Comput. Phys. Commun.* 178 (2008), pp. 852–867. DOI: 10.1016/j.cpc.2008.01.036. arXiv: 0710.3820 [hep-ph].

[24] Johan Alwall et al. "MadGraph 5 : Going Beyond". In: *JHEP* 06 (2011), p. 128. DOI: 10.1007/JHEP06(2011)128. arXiv: 1106.0522 [hep-ph].

[25] S. Agostinelli et al. "Geant4—a simulation toolkit". In: *Nuclear Instruments and Methods in Physics Research Section A: Accelerators, Spectrometers, Detectors and Associated Equipment* 506.3 (2003), pp. 250–303. ISSN: 0168-9002. DOI: https://doi.org/10.1016/S0168-9002(03)01368-8.

[26] G. M. Shore. "Superluminality and UV completion". In: *Nucl. Phys.* B778 (2007), pp. 219–258. DOI: 10.1016/j.nuclphysb.2007.03.034.

[27] C. Patrignani et al. "Review of Particle Physics". In: *Chin. Phys.* C40.10 (2016), p. 100001. DOI: 10.1088/1674-1137/40/10/100001.

[28] Vardan Khachatryan et al. "Searches for invisible decays of the Higgs boson in pp collisions at $\sqrt{s}$ = 7, 8, and 13 TeV". In: *JHEP* 02 (2017), p. 135. DOI: 10.1007/JHEP02(2017)135. arXiv: 1610.09218 [hep-ex].

[29] Matteo Cacciari, Gavin P. Salam, and Gregory Soyez. "The Anti-k(t) jet clustering algorithm". In: *JHEP* 04 (2008), p. 063. DOI: 10.1088/1126-6708/2008/04/063. arXiv: 0802.1189 [hep-ph].

[30] *Zero bias and HF-based minimum bias triggering for pp collisions at 14 TeV in CMS*. Tech. rep. CMS-PAS-QCD-07-002. URL: https://cds.cern.ch/record/1152558.

A Additional plots of semi-visible jet properties

The following figures are presented to support the inferences made into the kinematics of the s- and t-channel models.

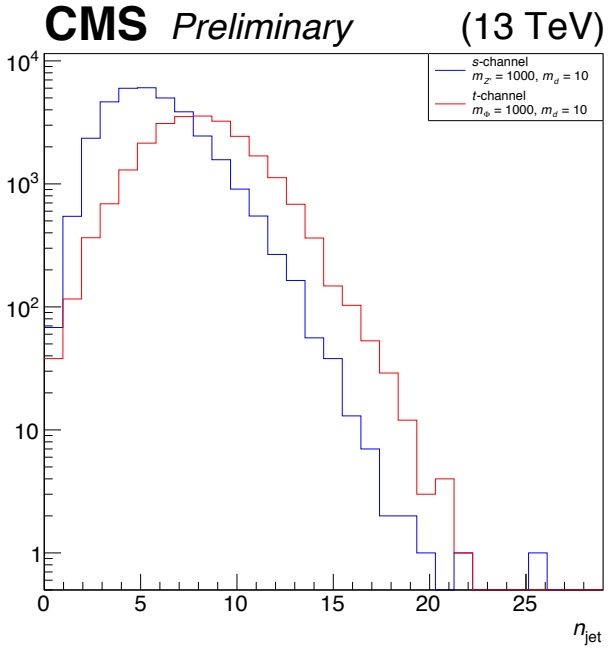

Figure 7: The distribution of the number of jets in the s- and t-channel semi-visible jet models with the following parameters: $m_{\text{med}} = 1000$ GeV, $m_d = 10$ GeV, $\Lambda_d = 10.5$ GeV and $r_{\text{inv}} = 0.3$.

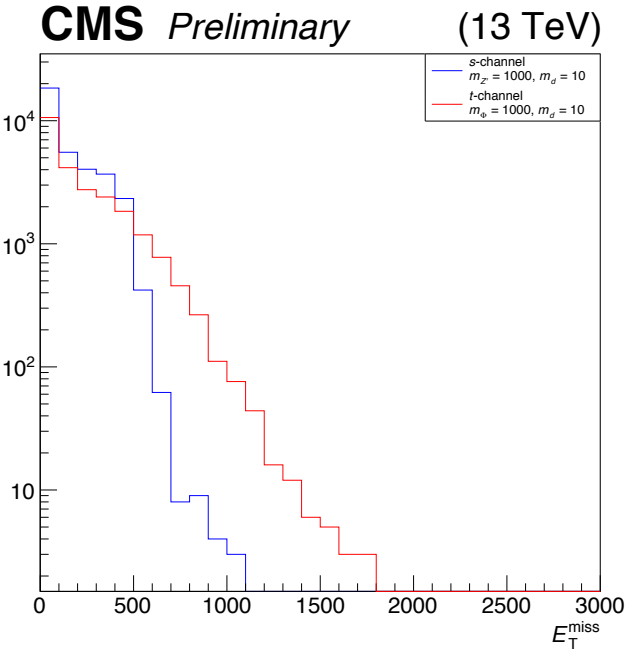

Figure 8: The distribution of $E_{\text{T}}^{\text{miss}}$ in the s- and t-channel semi-visible jet models with the following parameters: $m_{\text{med}} = 1000$ GeV, $m_d = 10$ GeV, $\Lambda_d = 10.5$ GeV and $r_{\text{inv}} = 0.3$.

B Feynman diagrams for $H \to$ inv. production modes

Below are some example Feynman diagrams for the $H \to$ inv. production modes discussed in the report.

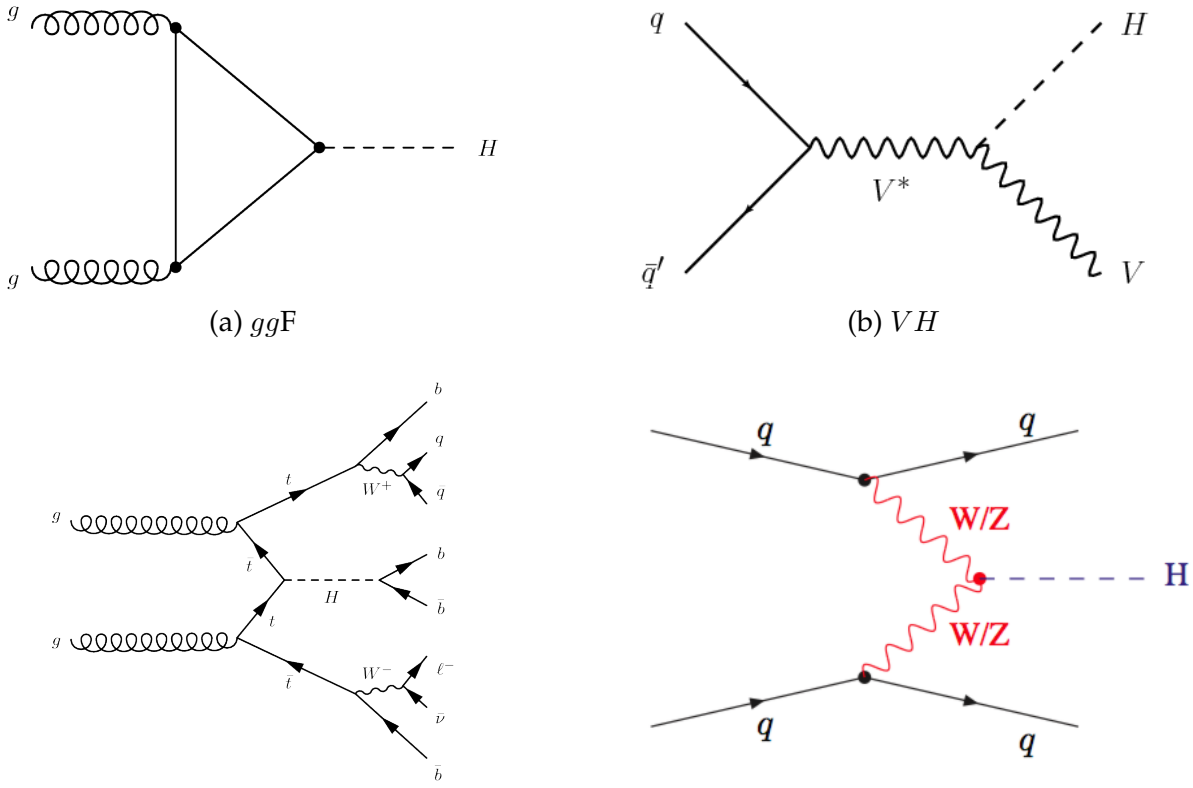

(a) ggF (b) VH

(c) ttH (d) VBF

Figure 9: A subset of the Feynman diagrams for some Higgs boson production modes.